Electronic Supplementary Material (ESI) for Journal of Materials Chemistry B.
This journal is © The Royal Society of Chemistry 2017

Electronic Supplementary Information

Defect engineered TiO_2 nanotube photonic crystals for fabrication of near-infrared photoelectrochemical sensor

Wenlong Wu, Zhonghai Zhang*

School of Chemistry and Molecular Engineering, East China Normal University, Dongchuan Road 500, Shanghai 200241, China

Address correspondence to zhzhang@chem.ecnu.edu.cn

Fig. S1-12

Reference list

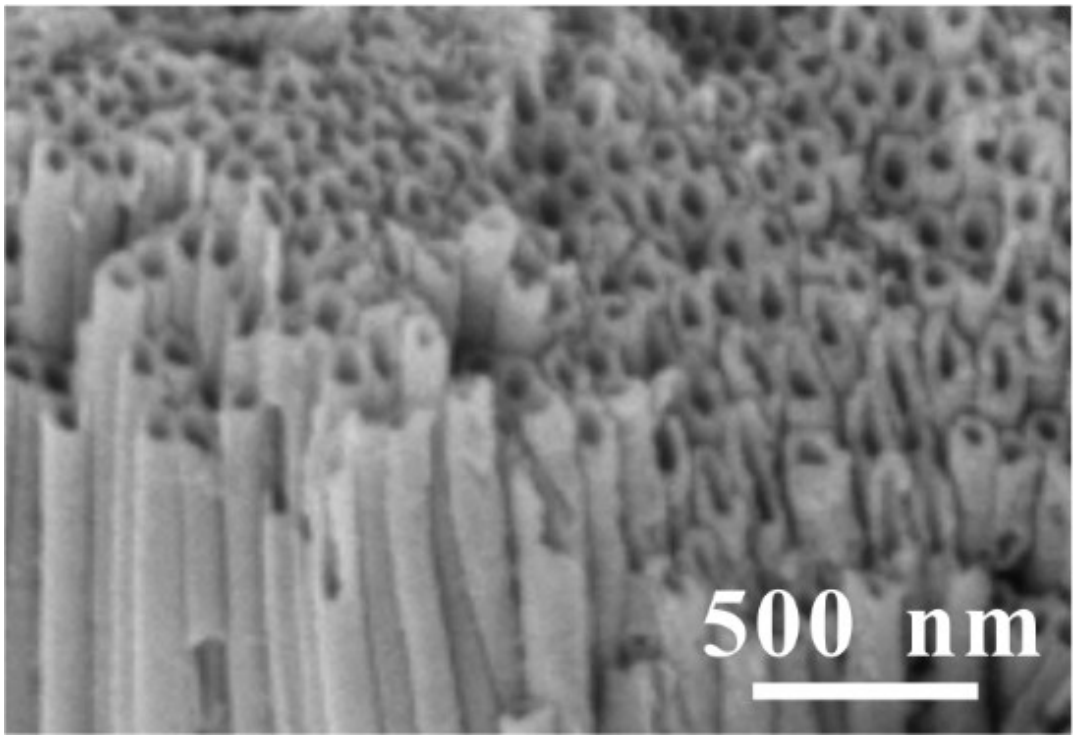

Fig. S1 Top-view SEM image of one-step anodized TiO_2 NTs.

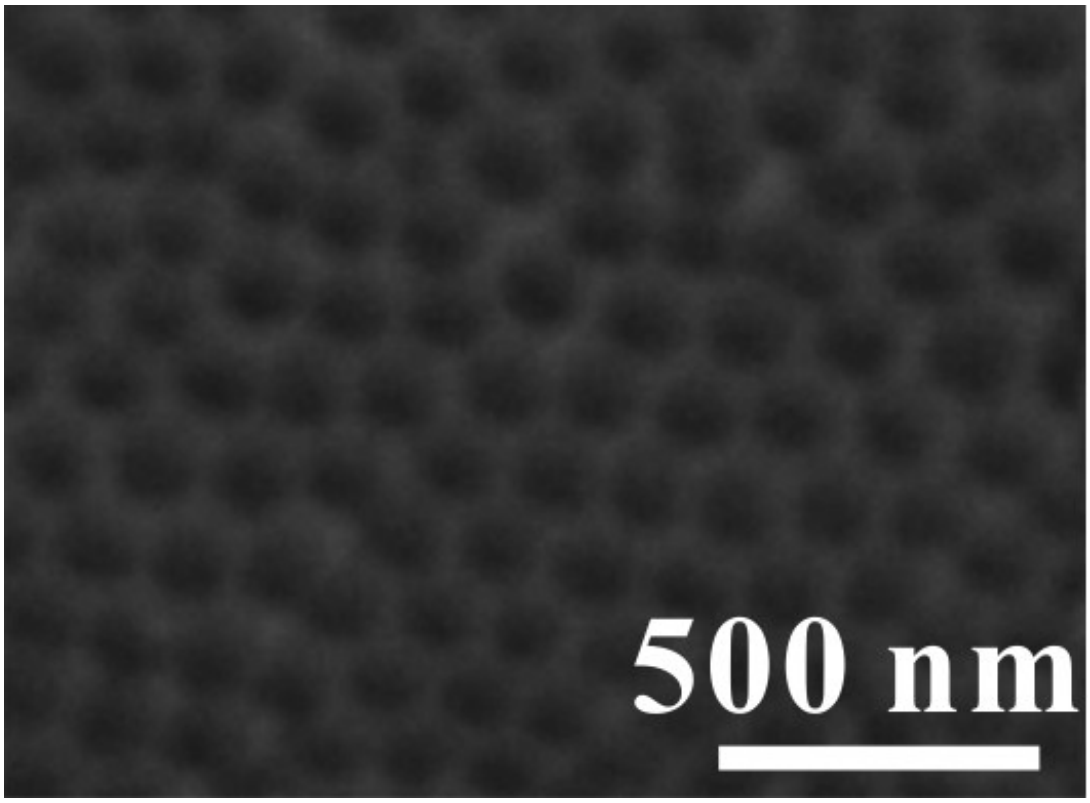

Fig. S2 Top-view SEM image of nanoconcaves.

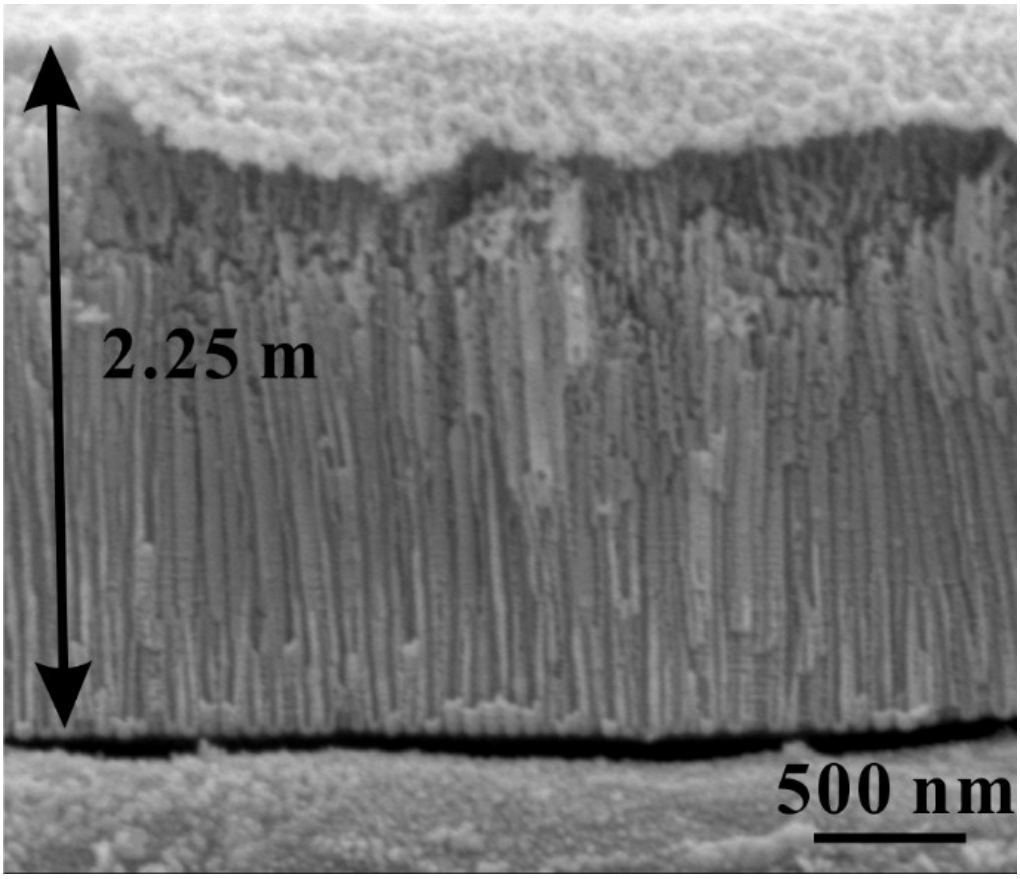

Fig. S3 Cross-sectional SEM image of TiO_2 NTPCs.

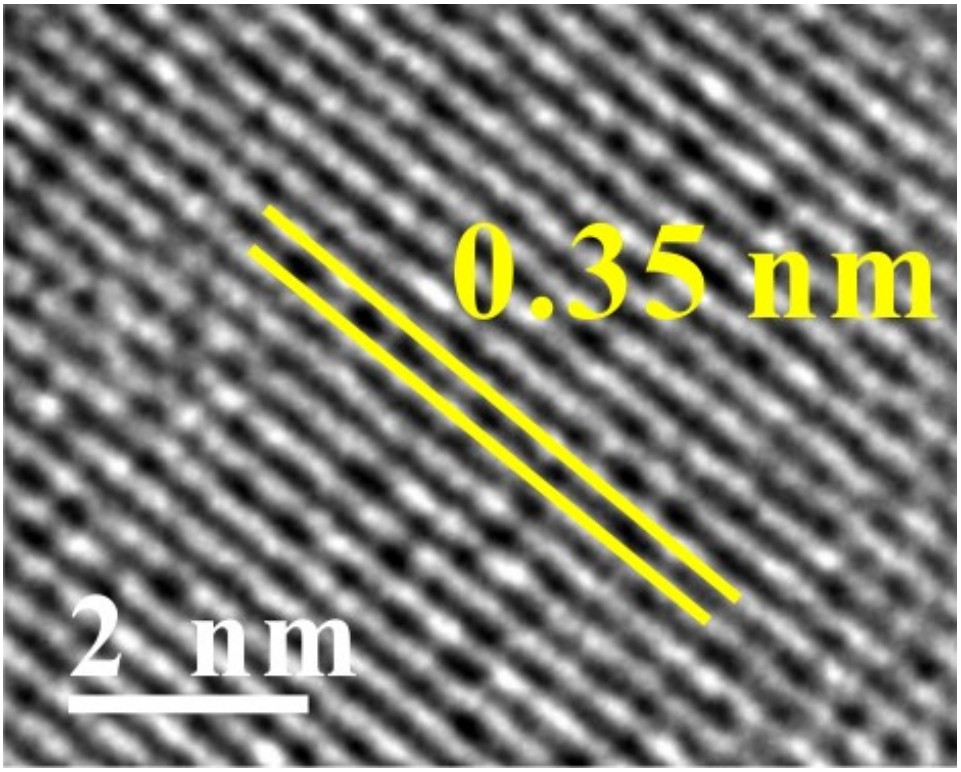

Fig. S4 HRTEM image of TiO_2 NTPCs.

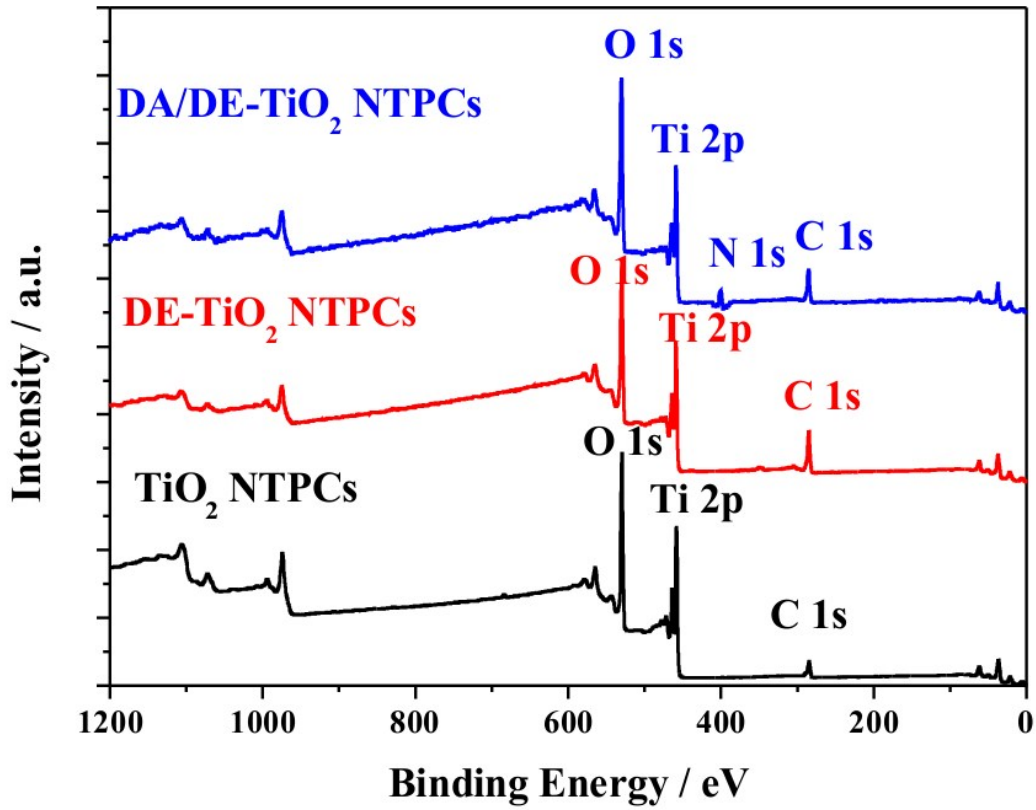

Fig. S5 XPS survey of TiO_2 NTPCs, DE-TiO_2 NTPCs, and DA/DE-TiO_2 NTPCs.

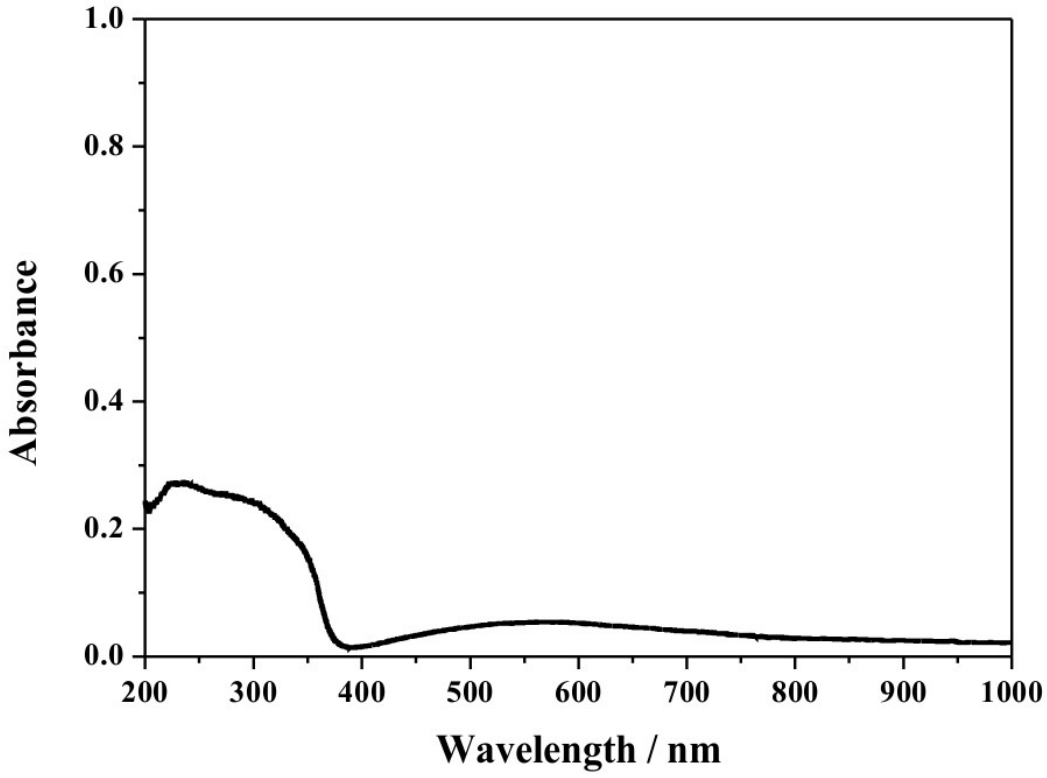

Fig. S6 DRS of TiO_2 NTs.

Fig. S7 Digital photos of (a) TiO_2 NTPCs and (b) DE-TiO_2 NTPCs.

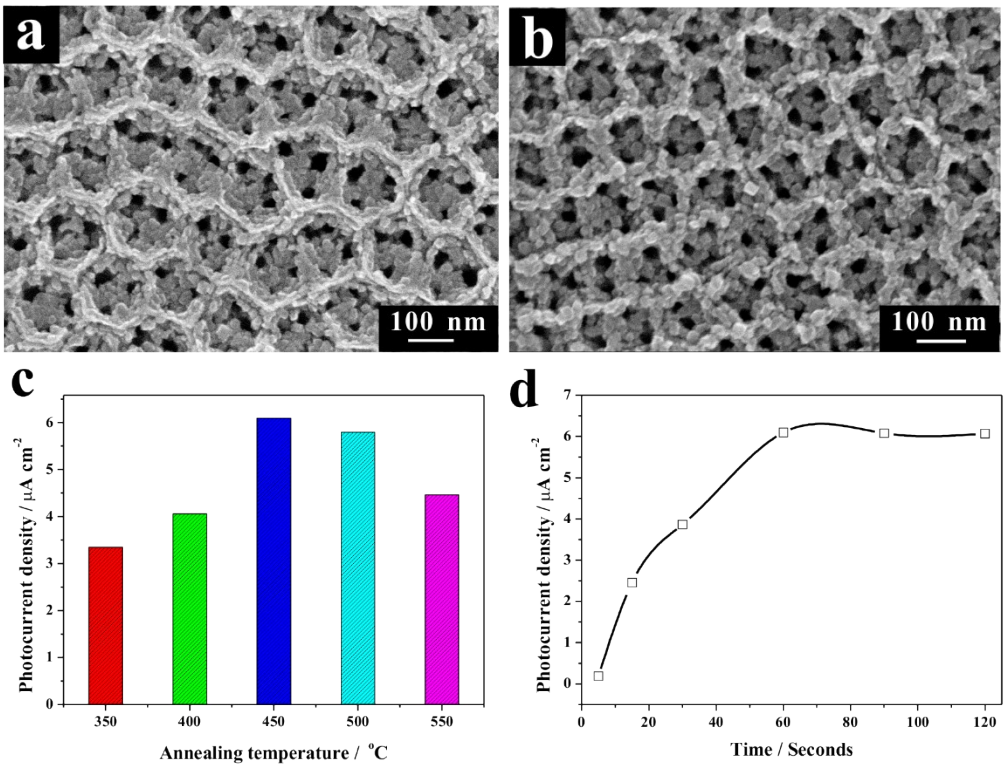

Fig. S8 Top-view SEM image of DE-TiO_2 NTPCs annealed at (a) 500 °C and 550 °C, (c) photocurrent density of DE-TiO_2 NTPs annealed at different temperature, and (d) photocurrent density of DE-TiO_2 NTPCs with different vacummized time.

The DE-TiO_2 NTPCs annealed at 350 °C and 400 °C showed similar morphologies

(no presented here) with DE-TiO_2 NTPCs annealed at 450 °C, further increased the temperature beyond 500 °C, the top ordered nanoring structure will be destroyed and loss the light harvesting ability (Fig. S8a,b), which will consequently decrease the NIR PEC performance (Fig. S8c). The vacummized time before annealing was also optimized, as showed in Fig. S8d, the DE-TiO_2 NTPCs presented steady PEC performance after 60 seconds vacummization. Thus the defect engineering condition is optimized to 60 seconds vacummization and 450 °C annealing.

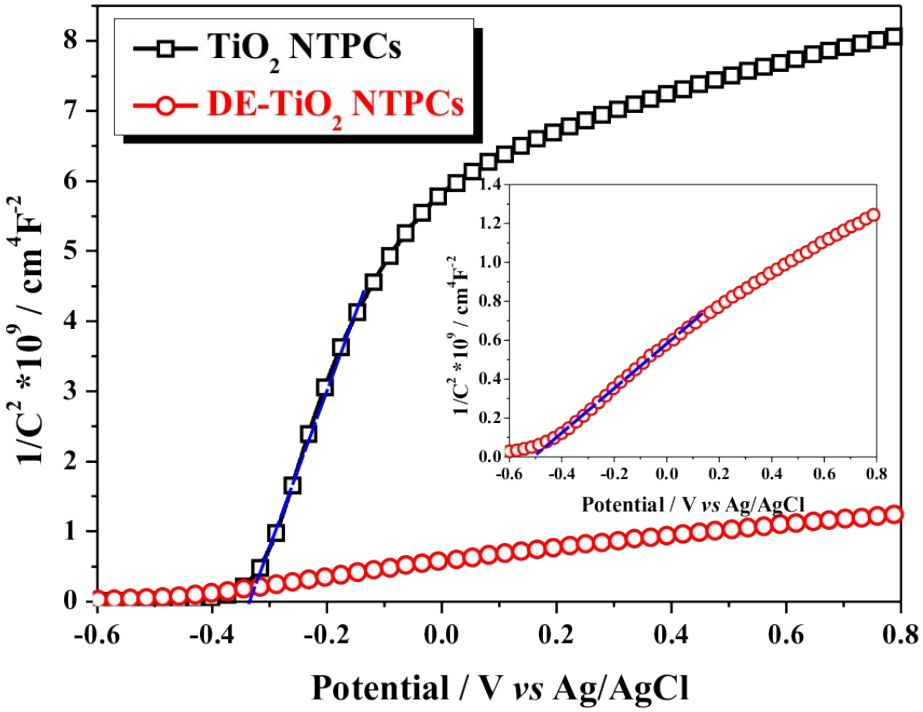

Fig. S9 Mott-Schottky plots of TiO_2 NTPCs and DE-TiO_2 NTPCs at a fixed frequency of 5 kHz, the inset is magnified plot of DE-TiO_2 NTPCs.

Mott-Schottky (MS) electrochemical impedance measurements were conducted in this study to display the capacitance change after defect engineering process. The MS plots of TiO_2 NTPCs and DE-TiO_2 NTPCs were presented in Fig. S9, and the semiconductor type, flat band potential (U_{FB}) and carrier density (N_D) were determined following the equation below:[1]

$$\frac{1}{C^2} = \frac{2}{N_D e \varepsilon_0 \varepsilon}[(U_S - U_{FB}) - \frac{k_B T}{e}] \quad (1)$$

where C is the space charge capacitance in the semiconductor; N_D is the electron carrier density; e is the elementary charge value; ε^0 is the permittivity of the vacuum; ε is the relative permittivity of the semiconductor; U_s is the applied potential; T is temperature; and k_B is the Boltzmann constant. The positive slopes of the linear part of the curves in MS plots indicated that the defect engineering did not change the n-type semiconductor property of TiO_2. The U_{FB} were estimated to be -0.33 V and -0.50 V for TiO_2 NTPCs and DE-TiO_2 NTPCs respectively. The negative shift of U_{FB} suggested steeper band bending, which would facilitate the charge separation at the semiconductor/electrolyte interface. The carrier density N_D was determined from Fig. S9 using the following equation:[1]

$$N_D = -\left(\frac{2}{e\varepsilon\varepsilon_0}\right)\left(\frac{d(1/C^2)}{d(U_s)}\right)^{-1} \quad (2)$$

with e = -1.6 × 10^{-19}, ε^0 = 8.86×10^{-12}, and ε = 48 for anatase TiO_2[2]. The pristine TiO_2 NTPCs showed a N_D of 1.5×10^{18} cm^{-3}, while the DE-TiO_2 NTPCs showed a much higher N_D of 2.4×10^{19} cm^{-3}.

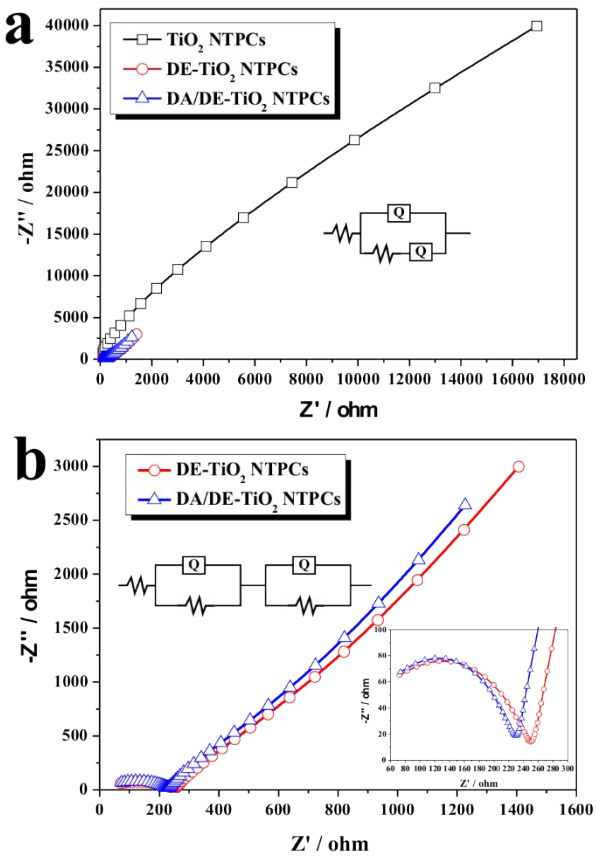

Fig. S10. (a) Electrochemical impedance spectra of TiO_2 NTPCs, DE-TiO_2 NTPCs, and DA/DE-TiO_2 NTPCs, (b) enlarged EIS of DE-TiO_2 NTPCs, and DA/DE-TiO_2 NTPCs, the insets are corresponding equivalent circuits.

Electrochemical impedance spectra (EIS) measurements were carried out for understanding the electronic modification after defect engineering process. As presented in Fig. S10a, the DE-TiO_2 NTPCs showed a much lower charge transfer resistance than TiO_2 NTPCs, implying the enriched defects (oxygen vacancies) significantly increased its electronic conductivity. The significantly enhanced electronic conductivity can be well explained from the increased carrier density (Fig. S9). After adsorption of DA on the surface of DE-TiO_2 NTPCs, a lower electron transfer resistance was also presented in Fig. S10b, which implied efficient charge transfer between DA and DE-TiO_2 NTPCs.

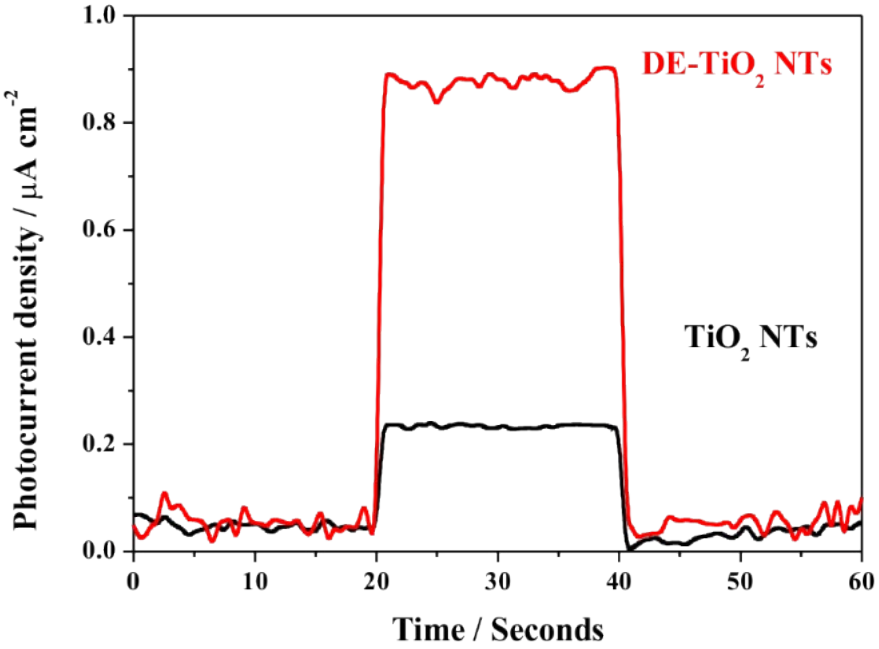

Fig. S11 PEC performance of TiO_2 NTs and DE-TiO_2 NTs under illumination of NIR light.

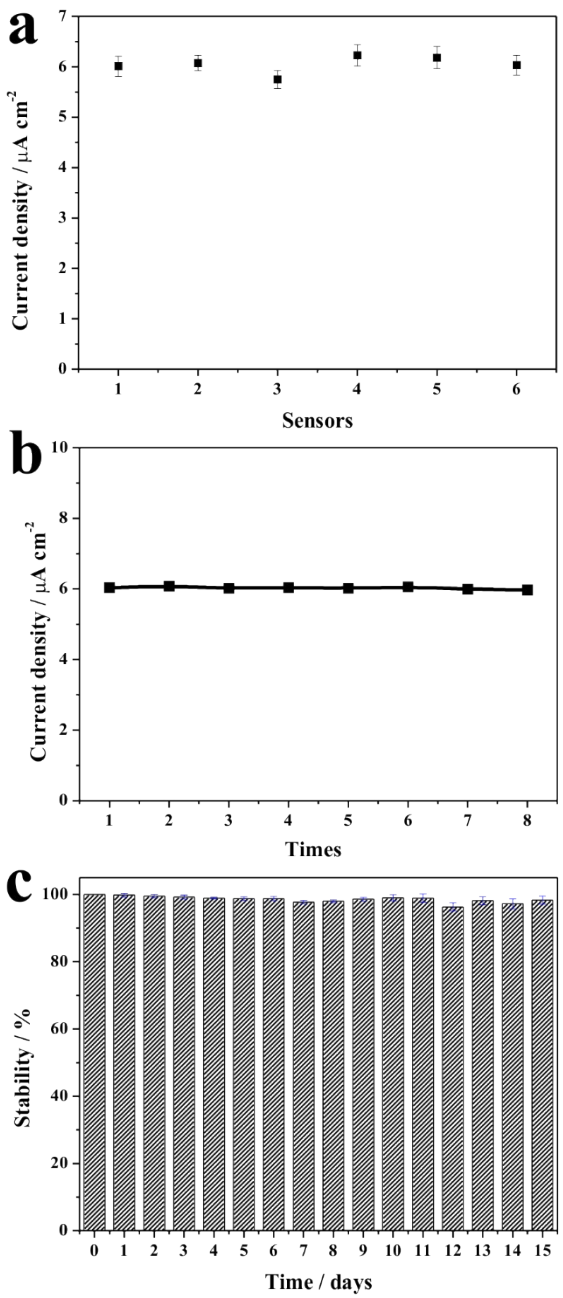

Fig. S12 Reproducibility, repeatability, and stability measurements of DE-TiO_2 NTPCs.

The detection reproducibility of batch sensors was investigated by measuring the response photocurrent of 6 photoelectrode, as shown in Fig. S12a, a relative standard deviation of 1.59% was achieved. The repeatability was measured with one electrode for 8 times and a relative standard deviation (RSD) of 2.27% was obtained (Fig. S12b).

Furthermore, the long-term stability of the PEC sensors was also tested by studying the current response intermittently in a period of 15 days (Fig. S12c), and no obvious photocurrent differences were found.

Reference list

1 G. Wang, H. Wang, Y. Ling, Y. Tang, X. Yang, R. C. Fitzmorris, C. Wang, Zhang, Z. J. Y. Li, *Nano. Lett.* **2011**, *11*, 3026.

2 Y. Xin, Z. Li, Z. Zhang, *Chem. Commun*. **2016**, *52*, 4541.